SINTER MORPHOLOGY AND THERMAL INFRARED IMAGERY: A DUAL APPROACH TO TRACKING HYDROTHERMAL CHANGES AROUND OLD FAITHFUL GEYSER, YELLOWSTONE, USA

Bridget Y. Lynne[1,2], Cheryl Jaworowski[3], Henry Heasler[3], Duncan Foley[4], Isaac Smith[2], Gary Smith[2]

[1]University of Auckland, 70 Symonds St, Auckland, New Zealand

[2] Geothermal Scientific Investigations Ltd, 11 Kyle Rd, Greenhithe, Auckland, New Zealand

[3] Independent Geologist, Powell, Wyoming, 82435

[4]Department of Geosciences, Pacific Lutheran University, Tacoma, WA USA 98447

b.lynne@auckland.ac.nz or bridget.lynn@gsilimited.com

Keywords: *Old Faithful Geyser, siliceous sinter, depositional processes, post-depositional overprinting, Thermal Infrared imaging.*

ABSTRACT

Geysers are among the world's most dynamic geothermal features. Our research, combining Scanning Electron Microscopy (SEM) with Thermal Infrared (TIR) imagery, demonstrates that Old Faithful Geyser in Yellowstone National Park, USA, varies at time scales well beyond eruption intervals. In 2015, we collected 13 siliceous sinter samples from the sinter apron surrounding Old Faithful Geyser, Yellowstone National Park, USA. These were the first sinter samples to be collected in 22 years from this area. Samples were examined using a Scanning Electron Microscope (SEM) to observe the sinter morphology. SEM results indicated three samples experienced on-going deposition of opal-A silica, while three other samples revealed intermittent deposition of opal-A silica. Four samples displayed mild, moderate or aggressive dissolution features indicating post-depositional overprinting via acidic steam condensate. One sample indicated both intermittent deposition of opal-A silica and dissolution textures. A further two samples revealed the sinter was altering to clay. We then compared the SEM information with calibrated and georectified 2007-2012 airborne night-TIR images. This dual process identified that samples in a northeast-southwest alignment have significantly higher ground temperatures than those indicated in the airborne night-TIR images. The combination of these unique samples with the publically available 2007-2012 airborne night-TIR images has provided useful information on the changing hydrology of the area surrounding Old Faithful Geyser.

1. INTRODUCTION

Located within Yellowstone National Park, USA, the world-iconic Old Faithful Geyser is part of the Upper Geyser Basin hydrothermal system. Several times a day, Old Faithful Geyser erupts, ejecting large quantities of alkali chloride water. The ejected water is either spewed into the air as droplets or discharged away from the vent along hydrothermal channels. Surrounding Old Faithful's vent is an expansive siliceous sinter apron.

Siliceous sinters are hot spring rocks. They form as near-neutral, alkali chloride hydrothermal water cools as it flows away from a vent and along a discharge channel. When the alkali chloride water temperature is less than 100°C, the non-crystalline opal-A silica carried in solution, precipitates out and accumulates to form siliceous sinter deposits (Fournier and Rowe, 1966; Weres and Apps, 1982; Fournier, 1985; Willimas and Crerar, 1985). Initially, the silica is deposited as well-rounded, opal-A spheres. The sinter deposit grows in vertical thickness and lateral extent as long as the silica-rich, alkali chloride water is discharging and wetting the sinter surface. The alkali chloride hydrothermal water is derived from a deep reservoir where the temperatures are higher than 175 °C (Fournier and Rowe, 1966).

Over time sinters undergo a series of silica phase transformations from non-crystalline opal-A to opal-A/CT to semi-crystalline opal-CT ± opal-C to crystalline quartz (Herdianita et al., 2000; Lynne et al., 2007). Sinter diagenesis is not time dependent and occurs with little or no burial. Post-depositional hydrothermal conditions can either accelerate or retard sinter diagenesis (Hinman, 1987, 1990, 1998; Campbell and Lynne, 2006; Lynne et al., 2005, 2006; Lynne, 2015).

Hydrothermal conditions can change over time from discharging alkali chloride water to steaming ground or fumarolic activity. Site-specific, post-depositional conditions can overprint previously formed sinter and these changes are recorded in the sinter morphology.

In April 2015, we collected 13 siliceous sinter samples from the sinter apron surrounding Old Faithful Geyser, to examine their morphology and compare their morphology with airborne night-TIR images from 2007-2012. This study is unique as these are the first siliceous sinter samples to be collected from the Old Faithful Geyser sinter apron in 22 years for SEM analysis.

ISSN 2703-4275

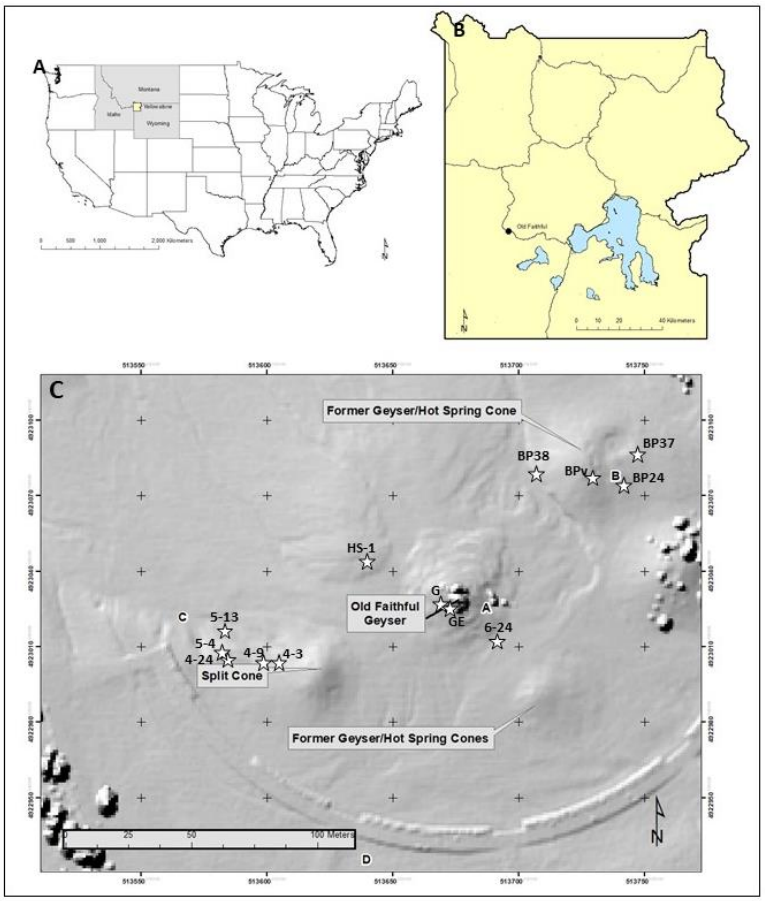

Figure 1: Location map of study area and sample sites. (A) Location of Yellowstone National Park. (B) Location of Old Faithful Geyser within Yellowstone National Park. (C) Sample sites shown on an NSF EarthScope 2008 LiDAR map of Old Faithful Geyser within Yellowstone National Park. A, B and C indicate the three sampled areas.

2. METHODS

2.1 Scanning Electron Microscopy

Thirteen samples were collected and analyzed using Scanning Electron Microscopy (SEM) to determine their morphological characteristics. The samples were mounted on aluminium stubs using epoxy. Samples were coated with platinum using a high-resolution Polaron SC7640 sputter coater. Samples were imaged using a Phillips (FEI) XL30S field emission gun SEM, at an accelerating voltage of 20 keV, and a working distance of 10 mm.

2.2 Calibrated Airborne Night-Thermal Infrared Imagery

Airborne night-thermal infrared (TIR) imagery of the Upper Geyser Basin, including the siliceous apron surrounding Old Faithful Geyser, were acquired, georectified and calibrated as part of a base-line study of the Upper Geyser Basin (Neale et al., 2016; Jaworowski et al., 2012). A series of calibrated, night-TIR imagery of the Old Faithful Geyser area from 2007-2012 forms a base-line.

High-elevation volcanic plateaus surround the hydrothermal basin (elevation 2246 m) that includes Old Faithful Geyser. The months of September and March are appropriate times for airborne night-TIR image acquisitions and the hydrothermal monitoring of the Old Faithful Geyser area. Table 1 contains the environmental conditions (air temperature (ºF), relative humidity (%), wind azimuth in degrees (o) and wind speed (m/s) at the time of image acquisitions in September and March.

Table 1: Environmental conditions during airborne night-TIR image acquisitions September 2007-March 2012. National Park Service data 2007-2011 at Old Faithful (AIRS Code: 56-039-1012) and 2012 from Lake weather stations.

Date	Time (a.m.)	Air Temp (ºF) or (°C)	Relative Humidity (%)	Wind (o)	Wind Speed (m/s)
12Sept 2007	2:23-2:36	21.2 or -6	14	235	4.2
12Sept 2008	1:04-1:21	16.4 or -8.7	29	261	2
11Sept 2009	3:29-3:41	20.7 or -6.2	19	360	1.5
25Sept 2010	12:58-1:09	3.3 or -15.9	93	121	0.4
9Sept 2011	2:51-3:02	3.3 or -15.9	71	143	0.6
3 March 2012	8:54 p.m.	-3.2 or -16	86	236	2.9

ISSN 2703-4275

3. RESULTS

SEM observations indicate two depositional and two post-depositional processes occurred in the siliceous sinter samples (Table 2).

Table 2: Processes observed under the SEM, in the siliceous sinter samples. On-going and intermittent deposition refer to deposition of opal-A silica.

Sample	Depositional process	Sample	Post-depositional process
6-24	On-going deposition	HS-1	Minor dissolution
4-9	On-going deposition	BP37	Minor dissolution
GE	On-going deposition	BP38	Moderate dissolution
5-13	Intermittent deposition	BPv	Moderate dissolution
G	Intermittent deposition	BP24	Aggressive dissolution
4-3	Intermittent deposition	5-4	Alteration to clay
HS-1	Intermittent deposition	4-24	Alteration to clay

3.1 Depositional processes

The SEM observations revealed two depositional processes taking place in the samples, as described below.

(1) On-going deposition of opal-A silica spheres: This process involves the continual deposition of numerous, well-rounded, opal-A spheres that range in size from <500 nm to ~2 µm. The different sized opal-A spheres form a thick groundmass with the smaller spheres being the youngest (Fig. 2). This process is enabled by the continual flow of silica-rich, alkali chloride water that has cooled to below 100°C.

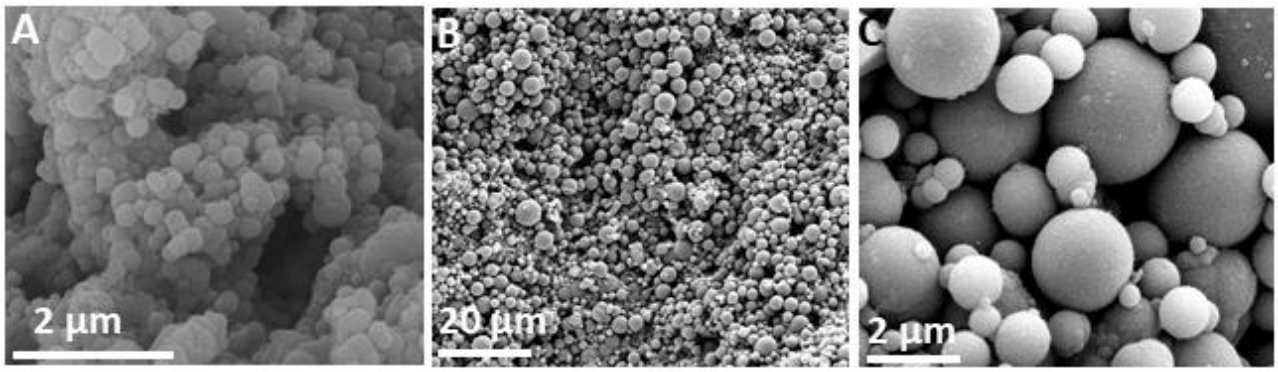

Figure 2: Ongoing deposition of multiple generations of opal-A spheres. (A) Sample 4-9. (B-C) Sample GE.

(2) Intermittent deposition of opal-A spheres: This process is due to intermittent flow of discharging alkali chloride water that cools to below 100°C. In these samples, newly-formed <1 µm diameter, opal-A spheres are deposited either: (a) in voids of previously formed smooth silica horizons (Fig. 3A); or (b) as newly-deposited <500 nm diameter opal-A spheres, that rest on previously-formed, botryoidal clusters of >2 µm diameter opal-A spheres (Fig. 3B-C).

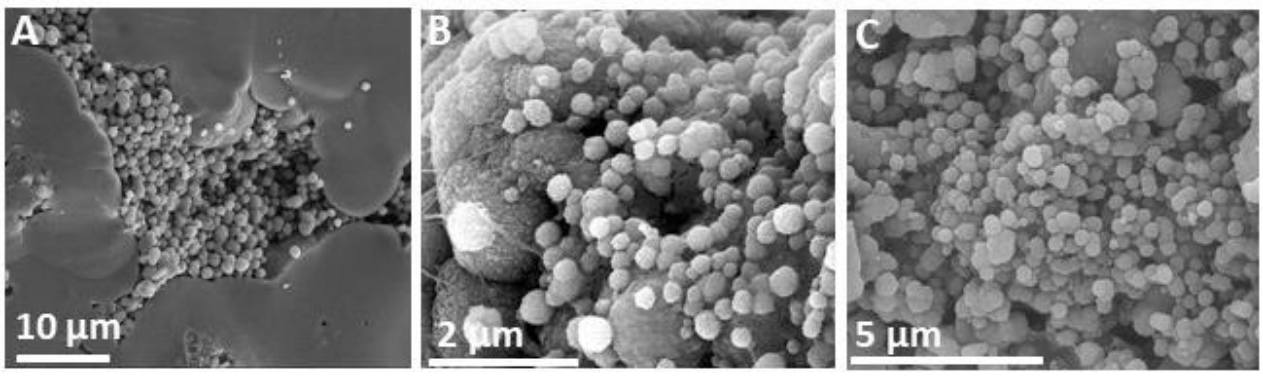

Figure 3: Intermittent deposition of opal-A spheres. (A) Sample 4-3 shows newly-formed opal-A spheres accumulated in void. Previously formed, botryoidal opal-A spheres occur around void rim. (B-C) Newly-deposited opal-A spheres on larger previously deposited opal-A spheres. (B) Sample G. (C) Sample 5-13.

ISSN 2703-4275

3.2 Post-depositional processes

Two post-depositional processes were observed in the samples. These processes include:

(1) Post-depositional dissolution processes caused by acidic steam condensate overprinting the siliceous sinter: A range of dissolution can be seen in our samples from minor to aggressive (Fig. 4). Minor dissolution is evident by the welding together of opal-A spheres (Fig. 4A). Moderate dissolution is observed as etched and pitted surfaces (Fig. 4B). Aggressive dissolution is shown in one sample where extensive etching and pitting of the sinter occurs, but also the early formation of quartz crystals can be seen psuedomorphing opal-A spheres (Fig. 4C).

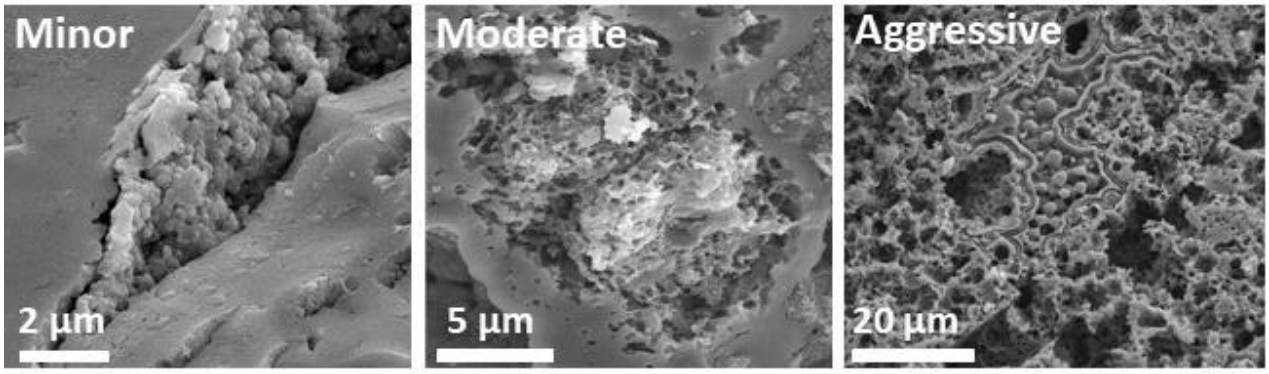

Figure 4: Dissolution processes range from minor to aggressive. Minor = sample HS-1. Moderate = sample BP38. Aggressive = sample BP24.

(2) Post-depositional alteration of siliceous sinter to clay: Alteration of sinter to clay was revealed in two samples. Sample 5-4 shows patches of clay platelets scattered over earlier formed, etched and pitted opal-A spheres (Fig. 5A). Clay has also formed in sample 4-24 where the clay platelets are better defined. In sample 4-24, multiple clay platelets almost cover the entire sinter surface (Fig. 5B).

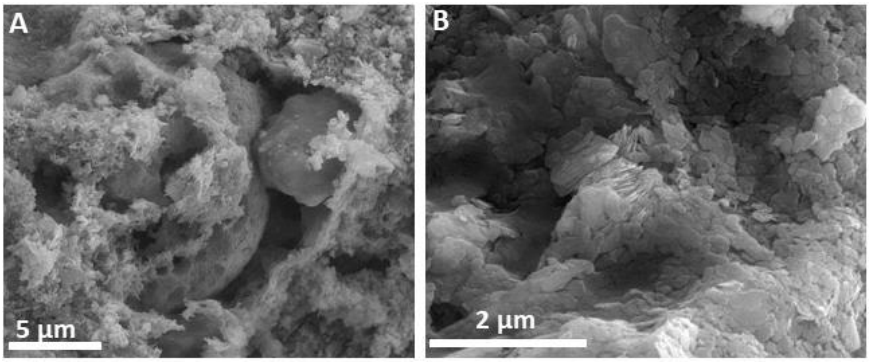

Figure 5: Post-depositional alteration of sinter to clay. (A) Sample 5-4. (B) Sample 4-24.

3.3 Calibrated Airborne Night-Thermal Infrared image comparisons to SEM processes

We plotted the sample locations onto publically available 2007-2012 night-TIR images (Fig. 6) and a 2008 LiDAR image. This enabled us to compare the ground surface temperature with the four processes recorded in our SEM images (Figs. 2-5). Table 3 summarizes our comparisons of the calibrated night-TIR temperatures and our SEM observations. In March 2012, air temperatures were -3.2ºF (-20ºC) at the time of airborne night-TIR image acquisition (see Table 1) in Yellowstone National Park. During the April 2015 field work and sample collection, daytime air temperatures varied between -3 to 8ºC. At times, during the 2015 field campaign, a dusting of snow covered the hydrothermally-influenced ground. Field observations of siliceous sinter showed polygonal patterns similar to patterned ground, indicating freeze-thaw processes are operating at the air-ground interface in the Upper Geyser Basin.

A sequence of calibrated September night-TIR images (2007-2012) provides a snapshot of the Old Faithful Geyser area over time (Fig. 6). Notice the variation in hydrothermal waters flowing west and northwest between 2007 and 2012. The arcuate 10-15ºC area (blue) to the south of an arcuate boardwalk is an area of obsidian sand that carries subsurface heat along buried infrastructure. The former geyser/hot spring cone northeast of Old Faithful Geyser consistently appears as a bright area on the night-TIR images. It is important to mention that the lowest temperature shown on the September night-TIR maps is 10ºC because there still may be a latent solar component in the lowest calibrated ground temperatures.

The calibrated, airborne March 2012 night-TIR image of the Old Faithful Geyser area provides a glimpse of the Old Faithful Geyser area after the Northern Hemisphere winter. Calibrated, ground temperatures lower than 10ºC reliably show hydrothermally influenced ground in the single digits on spring imagery. Therefore, the calibrated March 2012 night-TIR is the best image for comparing with the SEM evidence of depositional and post-depositional processes.

ISSN 2703-4275

3.3.1 On-going deposition of opal-A and TIR image

Sample sites GE, 6-24 and 4-9 were collected from flowing discharge channels. For these samples our SEM observations revealed the ongoing deposition of opal-A spheres. Between 2007 and 2012, calibrated, night-TIR temperatures at site 6-24 and 4-9 show the water temperature ranges from 4 to 15°C, while sample GE varies between 20-30ºC. The higher temperature at sample site GE may be attributed to its location beside the geyser vent.

3.3.2 Intermittent deposition of opal-A and TIR image

Four samples that indicate intermittent flow of alkali chloride water are samples G, 4-3, 5-13 and HS-1 Sample G, with night-TIR temperatures between 20 and 40°C is only 1 m from Old Faithful Geyser vent where the water is intermittently ejected at 92°C.

Sample 4-3 is close in proximity to sample 4-9 where we observed a discharge channel during our 2015 field work. Therefore, it is quite possible that sample 4-3 area is also intermittently covered in discharging alkali chloride water. Samples 4-9 and 4-3 both reveal the same 2012 night-TIR temperature of 6 °C. This heat is likely from discharging thermal water.

Sample HS-1 correlates to a calibrated 2007 to 2012 night-TIR temperature of 15 °C. SEM observations revealed minor dissolution as well as intermittent deposition of opal-A. Intermittent deposition of opal-A indicates this area is occasionally wet with alkali-chloride water, although the area was dry at the time of our field survey. The minor dissolution textures indicate alteration via acidic steam condensate. No steam was observed at this location during our field work. Given the freezing night-time temperatures in September and March, the night-TIR temperature of 15 °C suggests heat is transferred in the area. Given the presence of dissolution textures, the heat is more likely to be from steam discharge rather than a hot water discharge channel. The steam itself does not result in dissolution textures. It is the combination of hydrogen sulfide gas with the steam that creates acidic steam condensate that is responsible for dissolution textures.

Sample 5-13, with intermittent deposition of opal-A and no evidence of dissolution, correlates to calibrated 2007-2012 night-TIR temperatures of 15 to 30°C. In 2015, during our sample collection, no discharging steam was observed at this site. However, sample 5-13 was only 3 m from a discharge channel that was flowing during the 2015 field survey. Perhaps these night-TIR temperatures reflect flow of alkali chloride water at this location between 2007 and 2012, but the channel has since migrated.

3.3.3 Dissolution and TIR image

Samples BP37, BPv and BP24 revealed minor, moderate and aggressive dissolution textures respectively. These samples correlate to calibrated maximum night-TIR temperatures of 40°C (BP37), 20°C (BPv) and 30°C (BP24). SEM observations of these three samples suggest sinter overprinting by acidic steam condensate. During the field work, discharging puffs of steam and heat at the surface, was only noted at sample site BP24. The degree of post-depositional dissolution shown in the SEM images of these three samples suggest significant acidic steam condensate overprinting occurs at these locations.

3.3.4 Alteration to clay and TIR image

Samples 5-4 and 4-24 which revealed the sinter was altering to clay, are located within 5 m of each other. The calibrated, 2007-2012 airborne night-TIR image shows these samples correlate to a maximum ground surface temperature of 30°C (5-4) and 15°C (4-24). During our field work, occasional puffs of steam were observed at these two sample sites. For sinter to alter to clay, heat is required to dissolve the silica from the sinter and combined it with aluminum, probably from wind-blown soil particles, to form clay.

Table 3: Maximum night-TIR temperatures from 2007 to 2012 (calibrated and georectified) and processes identified by SEM. SEM process include: OG=on-going deposition. ID=Intermittent deposition. MiD=Minor dissolution. MoD=Moderate dissolution. AD=Aggressive dissolution. SC=Sinter altering to clay (Bold letters A, B and C refer to the three areas we collected samples from for this study).

	2007	**2008**	**2009**	**2010**	**2011**	**2012**	**SEM**
GE	30	30	30	20	30	30	OG
6-24	-	-	-	-	-	4	OG
4-9	-	-	-	15	15	6	OG
G	30	30	40	20	30	30	ID
4-3	-	-	-	-	-	6	ID
5-13	15	30	30	15	30	15	ID
HS-1	-	15	-	15	15	15	ID
HS-1	-	15	-	15	15	15	MiD
BP37	30	30	20	40	40	20	MiD
BP38	-	-	-	-	-	-	MoD
BPv	15	15	20	15	20	15	MoD
BP24	30	30	30	30	30	20	AD
5-4	-	15	30	-	20	6	SC
4-24	-	15	-	-	15	6	SC

ISSN 2703-4275

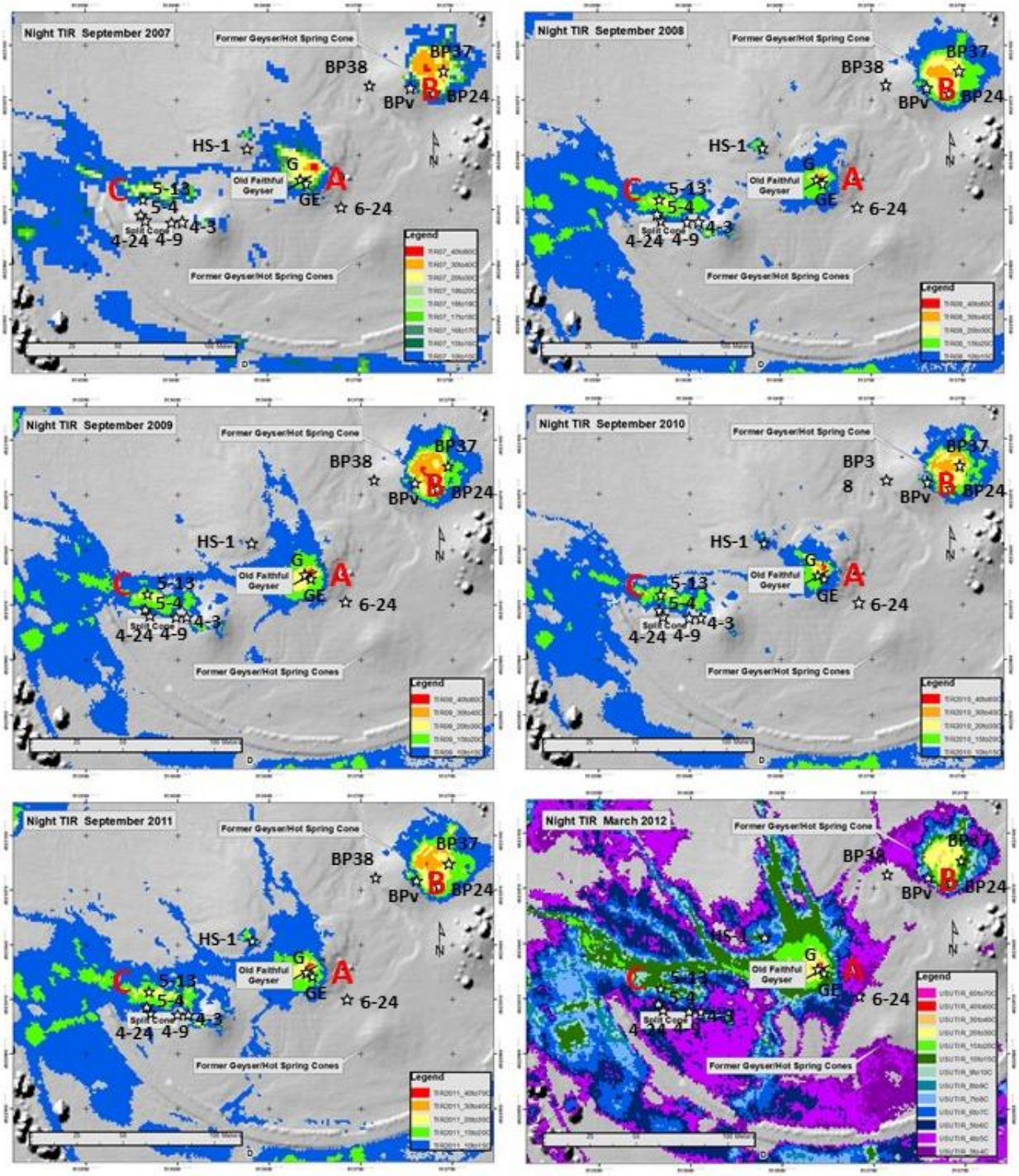

Figure 6. Sinter sample sites overlain on NSF-Earthscope LiDAR as well as calibrated and georectified 2007-2012 maps. Note that the night-TIR temperatures can be sliced into 1ºC increments. A, B and C indicate the three sampled areas.

The SEM results showed seven samples displayed either dissolution textures or alteration of sinter to clay. These seven samples form a northeast-southwest alignment from Split cone, flanking the Faithful Geyser vent, and ending at the former geyser/hot spring cone (Figure 7). For dissolution of the sinter or the formation of clay to occur, significant and prolonged quantities of acidic steam condensate would be required to overprint the sinter. A similar northeast-southwest alignment is seen as a broad (~ 80 m wide) northeast trend on the 2011 airborne night-TIR imagery and has been shown in previous work (Jaworowski et al., 2020). These seven samples also occur along northwest (HS-1 and BP 38) and west-northwest (5-4 and 4-24) trending night-TIR alignments. The west-northwest night-TIR alignment has been noted by Jaworowski et al. (2020) and corresponds to an area of hydrothermal clay minerals (Livo et al., 2007). It is possible that these seven samples also occur at the intersection of northeast and northwest fracture trends.

From the location of these seven samples on the 2012 night-TIR map, we can see that the temperatures vary from 3 to 6°C at the southwestern end of the alignment, to 6 to 15°C midway along the alignment and from 7 to 30°C at the northeast end of the alignment. This shows the 2012 night-TIR map detected an increase in temperature along the alignment from the southwest towards the northeast.

ISSN 2703-4275

By contrast, our SEM observations, identified aggressive post-depositional alteration of the sinter at both the southwest and northeast ends of the alignment, with minor dissolution midway along the alignment. These findings show how the combination of SEM with the night-TIR temperatures provide more detail on the hydrothermal setting and changing hydrology of the area.

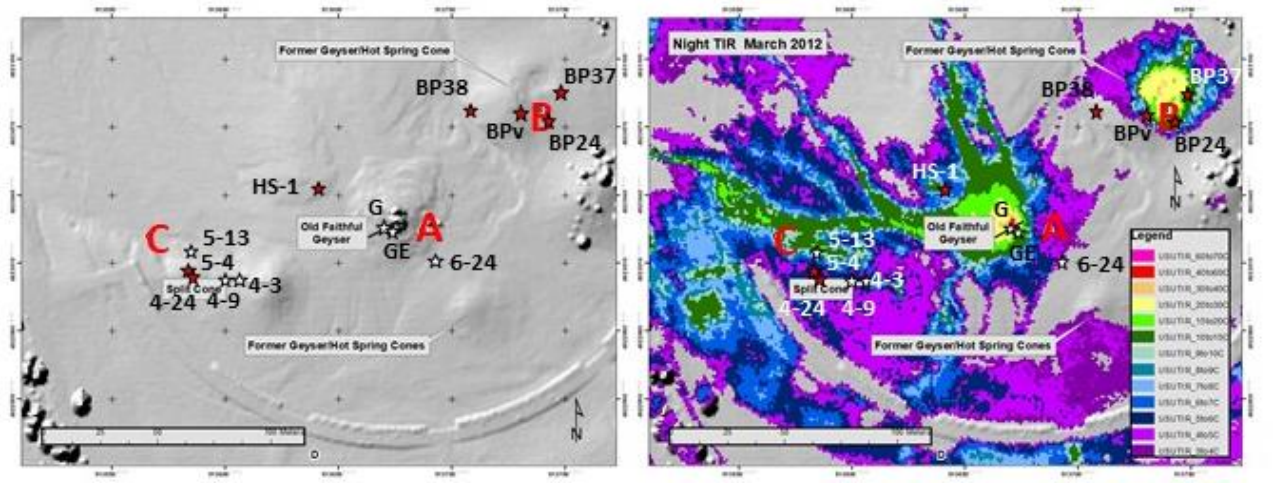

Figure 7: Sinter samples that revealed either dissolution textures or the formation of clay platelets (red stars). (A) NSF EarthScope 2008 LiDAR map of (B) calibrated and georectified airborne 2012 night-TIR over 2008 NSF-Earthscope LiDAR map.

4. DISCUSSION

Given two depositional and two post-depositional processes were noted over a distance of ~100 m from Old Faithful Geyser vent, it is evident that the local hydrothermal conditions vary over relatively small distances. The calibrated, airborne 2007-2012 night-TIR images document broad-scale, localized surface temperatures and provide a structural geolgic context, but do not provide information on near-surface processes. However, captured in the SEM images are both surface depositional processes and near-surface post-depositional. Documenting the spatial extent of near-surface significant heat in locations where aerial imagery shows minimal surficial heat, is valuable information as these areas are unstable and prone to subsidence. The comparaison of the calibrated, airborne night-TIR images with the SEM observations has provided a useful way to map the changing hydrothermal conditions surrounding the iconic Old Faithful Geyser.

It is well-documented that newly-formed siliceous sinter consists of opal-A, a non-crystalline silica phase (Smith, 1998; Herdianita et al., 2000). These SEM images confirm that the morphology of the newly-formed siliceous sinter surrounding Old Faithful Geyser looks identical to that which is widely reported around the world (e.g., Lynne et al., 2019; Smith et al., 2018; Nicolau et al., 2014).

Lynne et al., (2006) documented an experiment in a fumarolic setting in New Zealand, whereby they placed newly-formed opal-A siliceous sinter into a fumarole and recorded the mineralogical and morphological changes that took place within the sinter. The study documented that the acidic steam condensate setting overprinted the sinter and accelerated the diagenetic transformation of opal-A, directly to quartz. The BP24 sample also reveals the early formation of quartz crystals directly from opal-A spheres. However, the quartz crystals in our sample are more evident than those documented by Lynne et al., (2006). Furthermore, the sample indicates aggressive dissolution processes were in action, while Lynne et al., (2006) do not document dissolution of the opal-A sinter.

These SEM observations of siliceous sinter is an effective way to track sinter formation mechanisms and post-depositional hydrothermal conditions. When combined with calibrated, airborne night-TIR images, a better understanding of the changing hydrothermal conditions in a given area can be documented. Given access to Old Faithful Geyser and its surrounding sinter apron is extremely limited, these results contribute significant scientific information which improves the understanding of the hydrothermal conditions in the immediate vicinity of Old Faithful Geyser.

ACKNOWLEDGEMENTS

We thank the following for supporting this research: Expeditions Council of the National Geographic Society project ECO714-15, National Park Foundation Grant 9086, National Park Service Research Permit YELL-2014-SCI-5612, Rocky Mountain Cooperative Ecological Study Unit Agreements (RM-CESU J1580050583, J1580050608,and J1580090425) between Yellowstone National Park's Geology Program and Utah State University's Remote Sensing Services Laboratory, Geothermal Scientific Investigations Ltd, Pacific Lutheran University and the University of Auckland. We also thank our field crew and all the support personnel involved in making the acquisition of this data possible through collaboration of resources and expertise: specifically Dennis Lojko (Law Enforcement Ranger Yellowstone National Park), and Martin Gamache (National Geographic Magazine).

REFERENCES

Campbell, K.A. and Lynne, B.Y.: Diagenesis and dissolution at Sinter Island (456 years BP) Taupo Volcanic Zone: silica stars and the birth of quartz. In: *Proc. 28th New Zealand Geothermal Workshop*, 7 pp. (2006).

Fournier, R.O.: The behaviour of silica in hydrothermal solutions. *Reviews in Economic Geology*, 2, pp. 45-62. (1985).

Fournier, R.O., and Rowe, J.J.: Estimation of underground temperatures from the silica content of water from hot springs and steam wells. *Amercian Journal of Science*, 264, pp. 685-697. (1966).

Herdianita, N.R., Browne, P.R.L., Rodgers, K.A., Campbell, K.A..: Mineralogical and textural changes accompanying ageing of silica sinter. *Mineralium Deposita*, 35, pp. 48-62. (2000).

Hinman, N.W.: Organic and inorganic chemical controls on the rates of silica diagenesis, comparison of a natural system with experimental results. *PhD Thesis, La Jolla, University of California at San Diego*, 381 p. (1987).

Hinman, N.W.: Chemical factors influencing the rates and sequences of silica phase transitions: effects of organic constituents. *Geochemica et Cosmochemica Acta*, 54, pp. 1563-1574. (1990).

Hinman, N.W.: Sequences of silica phase transitions: effects of Na, Mg, K, Al and Fe ions. *Marine Geology*, 147, pp. 13-24. (1998).

Jaworowski, C., Lynne, B.Y., Heasler, H., Foley, D., Smith, I.J., Smith, G.J.: Detecting natural fractures with ground penetrating radar and airborne night-thermal infrared imagery around Old Faithful geyser, Yellowstone National Park, USA, *Geothermics* 85, pp. 1-11. (2020).

Jaworowski, C., Heasler, H.P., Neale, C.M.U., Sivarajan, S., Masih, A.: Monitoring the dynamic geohydrology of the Upper Geyser Basin Yellowstone National Park, In Neale, Cosh (eds.), *Proceedings of the International Commission on Remote Sensing of IAHS*, Jackson Hole, Wyoming, 27-30, September 2010, pp.54-58. (2012).

Livo, K.E., Kruse, F.A., Clark, R.N., Kokaly, R.F., Shanks III, W.C.: Hydrothermally altered rock and hot-spring deposits at Yellowstone National Park-characterized using airborne visible- and infrared spectroscopy data. In Morgan (Ed.), Integrated Geoscience Studies in the Greater Yellowstone Area-Volcanic, Tectonic, and Hydothermal Processes in the Yellowstone Ecosystem. *U.S. Geological Survey professional Paper 1717*, pp. 493-507. (2007).

Lynne, B.Y., Campbell, K.A., Moore, J.N., Browne, P.R.L.: Diagenesis of 1900-year-old siliceous sinter (from opal-A to quartz) at Opal Mound, Roosevelt, Utah, USA. *Sedimentary Geology*, 119, 249-278. (2005).

Lynne, B.Y., Campbell, K.A., Perry, R.S., Browne, P.R.L., Moore, J.N.: Acceleration of sinter diagenesis in an active fumarole, Orakei Korako, New Zealand. *Geology*, 34**,** 749-752. (2006).

Lynne, B.Y., Campbell, K.A., James, B.J., Browne, P.R.L., Moore, J.: Tracking crystallinity in siliceous sinters. *American Journal of Science*, 307, 612-341. (2007).

Lynne, B.Y.: Impact of three common post-depositional environmental settings on siliceous sinter diagenesis: An eight-year experiment *Journal of Volcanology and Geothermal Research*, 282, 84-101. (2015).

Lynne, B.Y., Boudreau, A., Smith, I.J., Smith, G.J.: Silica accumulation rates for siliceous sinter at Orakei Korako geothermal field, Taupo Volcanic Zone, New Zealand. *Geothermics*, 78, 50-61. (2019).

Neale, C.M.U., Jaworowski, C., Heasler, H., Sivarajan, S., Masih, A.: Hydrothermal monitoring in Yellowstone National Park using airborne thermal infrared remote sensing, Remote Sens. Environ. 184, 628-644. (2016).

Nicolau, C., Reich, M., Lynne, B.Y.: Physico-chemcal and environmental controls on siliceous sinter formation at the high-altitude El Tatio geothermal field, Chile. *Journal of Volcanology and Geothermal Research*, 282, pp. 60-76. (2014).

NSF EarthScope Intermountain Seismic Belt LiDAR Project, 2008, https://opentopography.org/, accessed 30 May 2021.

Smith, D.K.: Opal, cristobalite, and tridymite: noncrystallinity versus crystallinity, nomemclature of the silica minerals and bibliography. *Powder Diffraction*, 13, pp. 2-19. (1998).

Smith, I.J., Lynne, B.Y., Jaworowski, C., Qasim, I., Heasler, H., Foley, D.: The formation of geyser eggs at Old Faithful Geyser, Yellowstone National Park, USA. *Geothermics* 75, pp. 105-121. (2018).

Weres, O. and Apps, J.A.: Prediction of chemical problems in the reinjection of geothermal brines. *In: Marasimhan, T.N. (Ed.), Recent Trends in Hydrogeology. Geological Society of America*, Special Paper 189, pp. 407-426. (1982).

Williams, L.A., and Crerar, D.A.: Silica diagenesis, II: general mechanisms. *Journal of Sedimentary Petrology*, 55, pp. 312-321. (1985).

ISSN 2703-4275